Real time algorithms in the ATLAS tau trigger system at 7 TeV center of mass energy

P Kadlečík on behalf of the ATLAS Collaboration

Department of High Energy Physics, Niels Bohr Institute, Copenhagen University, Blegdamsvej 17, 2200 Copenhagen, Denmark

E-mail: kadlecik@nbi.dk

Abstract. The ATLAS hadronic tau trigger plays an important role in many analyses. Among these analyses are searches for H^0, $H^{\pm}$, W' and Z' in the tau decay channel. In order to achieve the needed sensitivity in these measurement it is important to reduce the QCD background, but at the same time to keep the signal efficiency high. Furthermore it is important to understand the trigger efficiency in real data. This paper summarizes the performance of the tau trigger in data collected by the ATLAS detector in 2011.

1. Introduction

The ATLAS tau trigger system is designed to select hadronically decaying taus while keeping the QCD jets at acceptable rates. The hadronic decays of the taus are identified by the track multiplicity as 1-prong (1 track, 76.5% of hadronic decays) and 3-prong (3 tracks, 23.5% of the hadronic decays). Unlike the QCD jets which have in general a high track multiplicity, the track multiplicity of the tau is low. Other characteristics of the taus are their narrowness and isolation. All the characteristics of the taus, narrowness, low track multiplicity and isolation are exploited by the tau trigger.

2. The ATLAS trigger

The Large Hadron Collider (LHC) provides proton-proton collisions at 40 MHz bunch crossing rate. The trigger system is designed to reduce the initial 40 MHz rate to an acceptable value which can be handled by the data acquisition system, by preselecting only the "interesting" events. The ATLAS trigger is a three level trigger system. The first level (L1) is a hardware-based trigger, while the Level 2 (L2) and Event Filter (EF) are software-based triggers. The L2 and EF triggers are often referred to as the Higher Level Trigger (HLT).

At L1, regions with high detector activity, the so called regions of interest (RoI's), are selected, which then seed the HLT. The trigger decision is based on the information contained in the RoI. The goal of L1 trigger is to reduce the initial 40 MHz rate to ∼75 kHz. The average processing time at L1 is ∼2 μs, which means that a decision on whether or not an event will be passed to the HLT, must be made within this time scale.

At L2 and at the EF sophisticated algorithms are used. The goal at L2 is to reduce the rate from ∼75 kHz to ∼5 kHz. The mean processing time at L2 is ∼40 ms. At L2, full granularity data inside the RoI is analyzed. The final rate reduction from 5 kHz to ∼200 Hz is done at the

EF. The events that have passed the L2 are analyzed at the EF using similar algorithms as run offline. The mean processing time at EF is ∼4 s.

The trigger bandwidths (L1 = 75 kHz, L2 = 5 kHz, EF = 200 Hz) at every trigger level are shared by a number of trigger items (for example electron, tau, muon, missing energy, calibration and detector performance trigger items). The rate of the trigger items can be controlled by the tightness of the trigger cuts, or by trigger prescales.

3. L1 tau trigger

The L1 tau trigger uses electromagnetic (EM) and hadronic (HAD) trigger towers of the size $\Delta\eta \times \Delta\phi = 0.1 \times 0.1$ for identifying the tau candidates, where η is the pseudorapidity[1] and ϕ is the azimuthal angle in the ATLAS detector.

The tau object at L1 is selected based on the requirements on the energy in the trigger towers of the size 2×2 in the calorimeter, the so called core region. The core region is surrounded by an isolation ring of 12 trigger towers, allowing to use isolation quantities at L1 if needed. The energy of the L1 tau object is calculated from trigger towers with the size 2×1 in the electromagnetic calorimeter[2], and the energy in the trigger towers with size 2×2 (full core region) in the hadronic calorimeter. The schematic view of the trigger towers can be seen in figure 1.

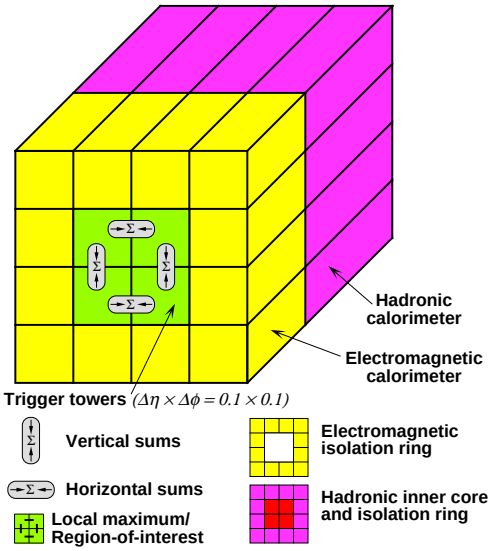

Figure 1. Simplified picture of the EM and HAD trigger towers showing the isolation (yellow and pink color) and the core region (green). The individual EM and HAD trigger towers are corresponding to the EM and HAD calorimeter cells (granularity: $\Delta\eta \times \Delta\phi = 0.1 \times 0.1$).

The rate of the L1 tau trigger items depends on the energy thresholds applied, and on the instantaneous luminosity. Some L1 items that have been deployed during the 2011 data taking are the L1_TAU6, L1_TAU8, L1_TAU11 and L1_TAU50. The number in the trigger name corresponds to the energy threshold of the L1 tau candidate in GeV. The rates of some of the L1 tau items, as a function of the instantaneous luminosity, are shown in figure 2. The tau trigger items presented in this paper did not require isolation at L1.

4. L2 tau trigger

The rate reduction at L2 is performed by defining and applying a selection based on variables, that are sensitive to the specific characteristics of the taus. The L2 tau candidate is reconstructed from calorimeter cells in the $\Delta\eta \times \Delta\phi$ =0.8×0.8 (Nor) region around the refined L1 direction. One of the most important variables, that uses the feature of the tau being narrower than the

[1] $\eta = -\ln\tan\frac{\theta}{2}$, where θ is the polar angle measured from the beam axis

[2] The electromagnetic calorimeter covers the layers 0 (presampler), 1, 2 and 3 of the ATLAS calorimeter [1].

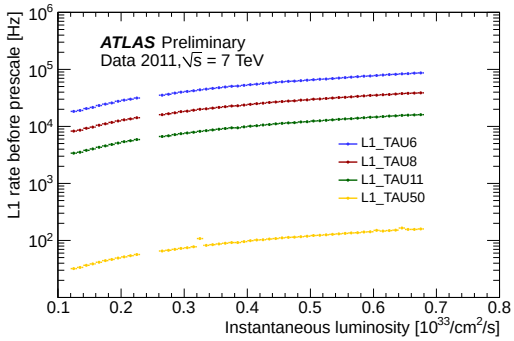

Figure 2. L1 rates before prescale versus the instantaneous luminosity measured by ATLAS for four different L1 tau items that are feeding primary HLT tau chains. The last digits in the L1 item name correspond to the transverse energy, E_{T}, requirement, e.g. a L1 $E_{\mathrm{T}} > 11$ GeV for L1_TAU11. The data has been collected in 14 runs at a centre-of-mass energy of 7 TeV in spring 2011.

typical QCD jet, is the electromagnetic radius, R_{EM}. It is an energy weighted radius in the Nor region calculated from cells in the EM calorimeter:

$$R_{\mathrm{EM}} = \frac{\sum_{Nor} E_{\mathrm{cell}} \Delta R_{\mathrm{cell}}}{\sum_{Nor} E_{\mathrm{cell}}}, \tag{1}$$

where $\Delta R_{\mathrm{cell}} = \sqrt{\Delta\eta^2 + \Delta\phi^2}$. $\Delta\eta$ and $\Delta\phi$ are the distances in the η and ϕ coordinates of the calorimeter cell with respect to the direction of the L2 tau candidate. E_{cell} is the energy of the calorimeter cell in the EM calorimeter.

Another variable that is used at L2 to reduce the rate is the transverse energy, E_{T}, of the L2 tau candidate. The L2 tau E_{T} is calculated from calorimeter cells inside the Nor region, and the suppression against the electronic and pile-up noise is applied.

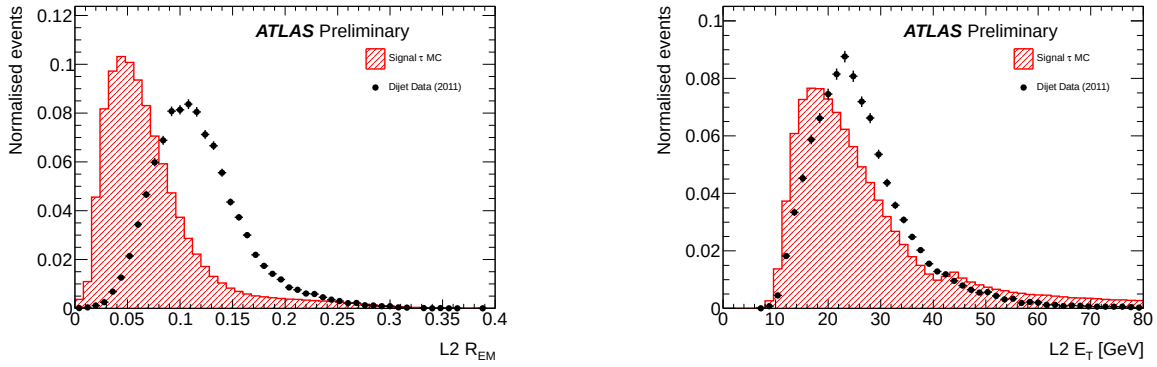

(a) (b)

Figure 3. Distributions of R_{EM} (a), and E_{T} (b) in a cone of radius 0.4 around the tau direction, at L2. The hatched histogram represents the combined contributions from $Z \to \tau\tau$, $W \to \tau\nu$ and $Z' \to \tau\tau$ signal Monte Carlo samples while the black points represent the data. A dijet selection has been applied to select the events in data.

The L2 distributions of R_{EM} and E_{T} for the QCD dijet events estimated from data and taus obtained from the Monte Carlo simulation are shown in figure 3(a) and (b). For the signal Monte Carlo distribution in figure 3, the L2 tau trigger candidates require to be associated with an offline tau candidate with $E_{\mathrm{T}} > 15$ GeV. For the dijet data in figure 3, the EF tau candidate is associated to an offline leading tau candidate with $E_{\mathrm{T}} > 30$ GeV, which is matched to a L1 tau RoI, and furthermore, the event must contain an additional subleading tau candidate with $E_{\mathrm{T}} > 15$ GeV.

5. EF tau trigger

At the EF we define various selection variables that take advantage of e.g. better tracking at the EF than at L2, or a better knowledge about the position of the trigger tau candidate. The EF tau candidate direction is reconstructed from calorimeter cells in the rectangular RoI, $\Delta\eta \times \Delta\phi = 0.8 \times 0.8$, centered around the L2 tau candidate direction. The EF tau candidate E_{T} is calculated from calorimeter cells within the RoI, centered around the refined EF tau candidate direction, applying electronic and pile-up noise suppression, and hadronic and tau specific energy calibration.

Tracks that are reconstructed at EF from inner detector hits by using a fast Kalman filter [2] are associated to the EF tau candidate within the region $\Delta\eta \times \Delta\phi = 0.4 \times 0.4$, centered around the L2 tau direction. For a track to be associated to the tau, the track must pass loose quality criteria including the cut on transverse momentum, $p_{\mathrm{T}} > 1$ GeV.

The selection that provides the rate reduction is parametrized as a function of transverse momentum of the EF tau candidate. Depending on the multiplicity of the tracks associated to the EF tau candidate, the selection is optimized for 1-prong (one associated track) and 3-prong (three associated tracks) taus separately.

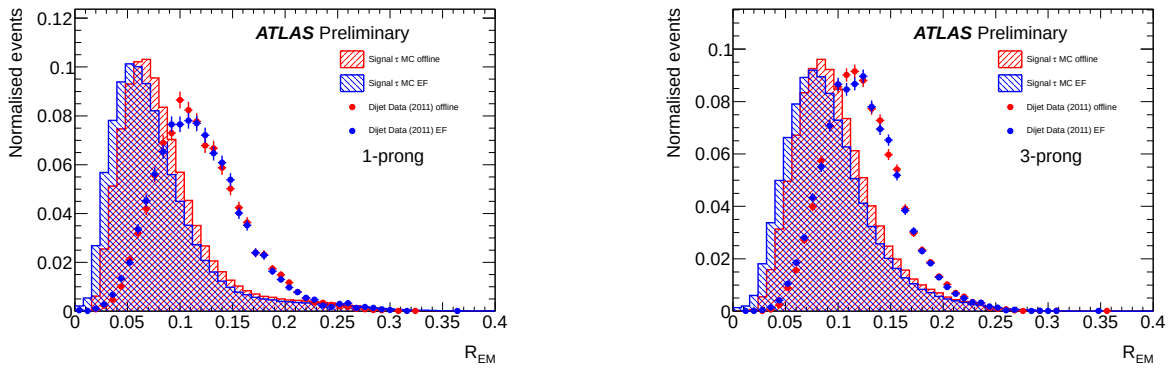

(a) (b)

Figure 4. In figures (a) and (b) are the distributions of radius of energy deposits in electromagnetic calorimeters, R_{EM}, for EF and offline reconstructed tau candidates with exactly 1 (a) and 3 (b) associated track(s). The hatched histogram represents the combined contributions from $Z \to \tau\tau$, $W \to \tau\nu$ and $Z' \to \tau\tau$ signal Monte Carlo samples while the points represent the data. A dijet selection has been applied to select the events in data. A less precise energy calibration applied at EF causes a shift on this distribution with respect to offline.

Calorimeter and track based variables are used to accept tau candidates. The most important calorimeter based variable is R_{EM}, which is defined at EF similarly as at L2, but takes advantage of the refined position of the EF tau candidate. The distributions of R_{EM} for 1-prong and 3-prong tau candidates at the EF are shown in figure 4, for signal Monte Carlo (which is the combination of $Z \to \tau\tau$, $W \to \tau\nu$ and $Z' \to \tau\tau$) and for dijet sample selected from data. In figure 4, the EF tau candidates in data and in Monte Carlo have to be associated with the offline tau candidates with the same requirements as mentioned in the discussion to figure 3. A good agreement between EF and offline variables is observed in both Monte Carlo and in data.

6. Tau trigger performance and analyses using the tau trigger in 2011

The tau trigger in combination with missing E_{T} trigger has been successfully used in 2010 for the observation of the $W \to \tau\nu$ events [3] and in 2011 for the $W \to \tau\nu$ cross section measurement

[4]. In 2011, the tau items have been used in combinations with other trigger items such as with muon trigger (shortly denoted as "mu"), electron trigger ("e"), missing E_{T} trigger ("xe"), or jet trigger ("j"), in various physics analyses.

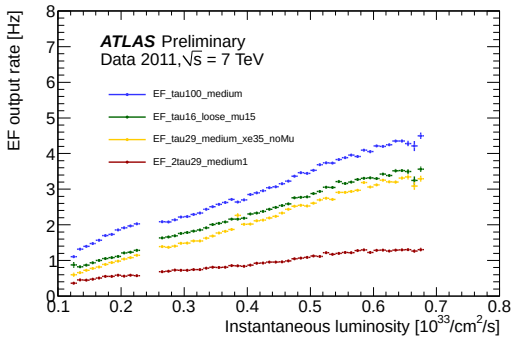

Figure 5. EF output rates versus the instantaneous luminosity of four different trigger items, each including at least one tau trigger.

Figure 5 shows the rates at EF as a function of the instantaneous luminosity in early 2011 runs of four tau (and combined) trigger items: EF_TAU100_MEDIUM, which is a single trigger item that requires at EF a tau with $E_{\mathrm{T}} > 100$ GeV and medium identification requirements; EF_TAU16_LOOSE_MU15, which is a combined trigger that requires at EF a tau with $E_{\mathrm{T}} > 16$ GeV and with loose identification requirements, and a muon with $p_{\mathrm{T}} > 15$ GeV; EF_TAU29_MEDIUM_XE35_NOMU, which is a combined trigger requiring at EF a tau with $E_{\mathrm{T}} > 29$ GeV and medium identification requirements, and missing E_{T} greater than 35 GeV; 2EF_TAU29_MEDIUM1, which is a combined trigger requiring two taus at EF, both with E_{T} greater than 29 GeV and both passing medium identification requirements with strict requirement on the number of tracks associated to the tau trigger object. The identification requirements (loose and medium) at the trigger level are similar to the offline tau identification requirements, but applying looser cut values due to the resolution effects.

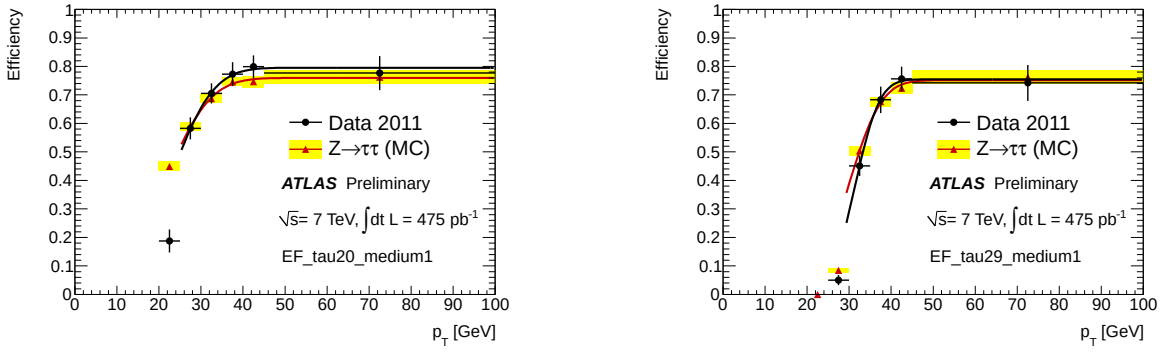

(a) (b)

Figure 6. Efficiency of the EF_TAU20_MEDIUM1 (a) and EF_TAU29_MEDIUM1 (b) trigger with respect to offline reconstructed tau candidates, as a function of the offline p_{T}. The tau candidates are required to pass medium identification criteria and include a strict requirement on the number of tracks associated to the trigger object.

The measurement of the trigger efficiency in the 2011 data has been done using a tag and probe analysis with $Z \rightarrow \tau\tau \rightarrow \tau_{\mu}\tau_{had}$ events. A single lepton trigger has been used to tag

the events in data, while measuring the tau trigger efficiency of the probed τ_{had}. The event selection followed closely the selection used in the $Z \to \tau\tau$ cross section measurement described in [5]. In this way it was possible to measure the trigger efficiency of some tau items in a data driven way. The comparison of the trigger turn on curves in data and in $Z \to \tau\tau$ Monte Carlo is shown in figure 6(a) for EF_TAU20_MEDIUM1, and in (b) for EF_TAU29_MEDIUM1 item. A good agreement of data and Monte Carlo has been observed.

7. Conclusions

In 2010 the tau trigger has been successfully commissioned and fully operational in 2011. During the 2011 data taking more than 5 fb^{-1} of real data has been collected by ATLAS at $\sqrt{s} = 7$ TeV. With this amount of data we will be able to provide many exciting analyses and the tau trigger in many of those will play an important role. The results we have obtained so far have given confidence about the performance of the tau trigger. The future improvements of the tau trigger involve using a selection more robust against the pile-up and multivariate methods at the EF.

References

[1] The ATLAS Collaboration *et al* 2008 The ATLAS Experiment at the CERN Large Hadron Collider *JINST* **3** S08003.

[2] Fruhwirth R 1987 Application of Kalman filtering to track and vertex fitting. *Nucl. Instrum. Methods* A 262 444

[3] The ATLAS Collaboration *et al* 2010 Observation of $W \to \tau\nu$ Decays with the ATLAS Experiment *Preprint* ATLAS-CONF-2010-097

[4] The ATLAS Collaboration *et al* 2012 Measurement of the $W \to \tau\nu$ Cross Section in pp Collisions at $\sqrt{s} = 7$ TeV with the ATLAS experiment *Phys. Lett.* B **706** 276-294

[5] The ATLAS Collaboration *et al* 2011 Measurement of the $Z \to \tau\tau$ Cross-Section with the ATLAS Detector *Phys. Rev.* D **84** 112006